Flapping Wing Flight Can Save Aerodynamic Power Compared to Steady Flight

Umberto Pesavento and Z. Jane Wang*

Department of Theoretical and Applied Mechanics, Cornell University, Ithaca, New York 14853, USA
(Received 6 April 2009; published 11 September 2009)

Flapping flight is more maneuverable than steady flight. It is debated whether this advantage is necessarily accompanied by a trade-off in the flight efficiency. Here we ask if any flapping motion exists that is aerodynamically more efficient than the optimal steady motion. We solve the Navier-Stokes equation governing the fluid dynamics around a 2D flapping wing, and determine the minimal aerodynamic power needed to support a specified weight. While most flapping wing motions are more costly than the optimal steady wing motion, we find that optimized flapping wing motions can save up to 27% of the aerodynamic power required by the optimal steady flight. We explain the cause of this energetic advantage.

Birds and insects have evolved to fly with flapping wings. Planes are designed to fly with fixed wings. These different styles of flight result from the complex evolutionary history of animals and machines, and as such cannot be entirely explained by aerodynamics. Nevertheless, the coexistence of these strikingly different flight styles motivates us to ask whether one of them is aerodynamically more advantageous than the other. There are reasons to argue for different answers. First, noting the complex flow created by flapping wings [1,2], we could argue that flapping flight appears to waste energy in churning up the flow and thus is less efficient. Alternatively, noting that fixed and flapping wings are employed at different scales, we could argue that fixed wing flight is more efficient at larger scales, and flapping flight at smaller scales.

Recent experimental and computational studies have examined the effects of various parameters on the force and power production in flapping flight, finding various local optima [3–7]. Since there is no general method to determine the global optimal solution, these local optima of flapping flight are not guaranteed to be efficient. For example, the much-studied generic translational and pitching motion with sinusoidal time variations is typically less efficient than the optimal steady motion of the same wing (Fig. 1). In practice, we find that most prescribed flapping motions are less efficient than the optimal steady motion. This can be understood in the quasisteady limit, in which the efficiency is determined only by the angle of attack. In such a regime, a steady wing can operate constantly at the optimal angle of attack, whereas a flapping wing periodically deviates from it and therefore is less efficient. The same general results can be confirmed by analyzing a two-stroke flapping motion [8]. Without unexpected unsteady effects, a flapping wing is always less efficient. In this sense, the optimal fixed wing motion sets a high bar to measure the cost of the flapping wing motion against. Therefore, instead of showing that the found solutions are optimal in the global sense, which is impractical for

these problems, we show that the new solutions outperform the previously known best solutions.

The goal of this work is to identify at least one case in which unsteady aerodynamics makes a flapping motion less costly than the optimal steady wing motion. We compare the aerodynamic power needed to overcome the fluid drag and support a given weight using either steady or flapping motions. This is measured by the dimensionless quantity P^*, defined as

$$P^* = \frac{\int_0^T [\vec{F}(t) \cdot \vec{U}(t) + \vec{\tau} \cdot \vec{\Omega}(t)] dt}{MgTU_{\text{ref}}}, \quad (1)$$
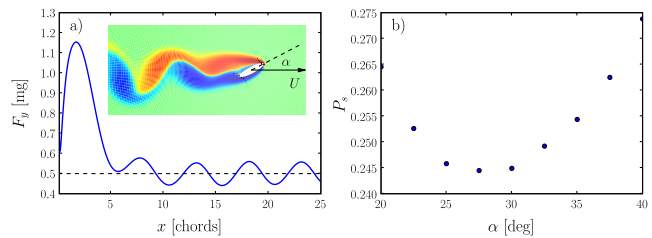
with the constraint

FIG. 1 (color online). Optimization of fixed wing kinematics for a wing of elliptical cross section of aspect ratio 1/4 and chord length 6.8×10^{-2} cm. (a) Vertical force F_y as a function of the distance traveled at the optimal angle of attack. In the inset, vorticity field around the wing at steady state. (b) Specific power as a function of the angle of attack α. For each α, the velocity is chosen to support a weight of 0.5 mg at steady state. In the range of between 20° and 40°, containing the optimal angle of attack, the flow around the wing is separated, exhibiting dynamic stall followed by periodic vortex shedding. The minimum specific power $P_s = 0.245$ occurs at a velocity of 2.94 m/s and an angle of attack of 27.5°. Each data point is obtained by averaging several periods after the flow has reached a periodic state. The numerical convergence of each simulation is checked by comparing computations using a 128×256 grid and a 256×512 grid.

$$\frac{1}{T} \int_0^T \vec{F}(t) \cdot \hat{z} dt = Mg, \qquad (2)$$

where $\vec{F}(t)$ and $\vec{U}(t)$ are instantaneous aerodynamic force and wing translational velocity, respectively. $\vec{\tau}(t)$ and $\vec{\Omega}(t)$ are the instantaneous aerodynamic torque and wing angular velocity, Mg is the weight, and T is the period. P^* is dimensionless, and the reference velocity $U_{\text{ref}} = \sqrt{\frac{2Mg}{\rho A}}$ is constant for a specific wing of area A and weight Mg. We note that in the case of steady wing motion with a constant angle of attack, the lift and drag are proportional to U^2, and it follows that $P^* = C_D(\alpha)/C_L^{3/2}(\alpha)$, where $C_L(\alpha)$ and $C_D(\alpha)$ are lift and drag coefficients at an angle of attack α, respectively.

We fix the shape of the wing and the weight, and seek the wing motion that minimizes the aerodynamic power subject to the weight balance constraint. Although it is possible to compute 3D flows around 3D rigid or flexible wings [9–11], the computational cost of such simulations would limit the number of trials allowed in the optimization procedure. A 3D simulation on 128^3 grid takes about 50 h to simulate 5 periods on a typical desktop computer [11], which makes optimization task unrealistic. Instead, by using 2D computations we are able to carry out an optimization of the unsteady flows around flapping and fixed wings at Re ~ 100. Specifically we compute the aerodynamic power of a 2D rigid wing with elliptical cross section and aspect ratio $1/4$ undergoing a prescribed motion by solving the Navier-Stokes equation [12,13]. The optimizations described here were performed using a 256×512 grid. Qualitatively similar results are obtained with a 125×256 grid. To verify the convergence of these results, simulations were repeated with a 512×1024 grid for the parameters corresponding to local optima. To choose meaningful parameters for our calculation, we base the morphological parameters on those of a fruit fly (see the caption of Fig. 2).

In order to solve the constrained minimization problem described above, we use a derivative-free method and take advantage of a quasisteady model to improve its speed of convergence. We discretize the phase space representing the kinematics in all dimensions except for the flapping frequency (or the velocity, in the case of a stead wing). At each point in the discretized space, we first solve the force balance constrained by tuning the frequency of motion. We start by choosing the frequency of motion which satisfies the constraint for the quasisteady model in which the aerodynamic lift is quadratic with respect to the wing velocity and varies as $\sin 2\alpha$ with the angle of attack α [13]. We then calculate a Navier-Stokes solution for the corresponding wing motion. If the resulting force does not satisfy the constraint balance, we use the previous Navier-Stokes solution to obtain a better estimate of the dimensionless constant of the quasisteady model, and we repeat the procedure until the constraint is satisfied by the Navier-
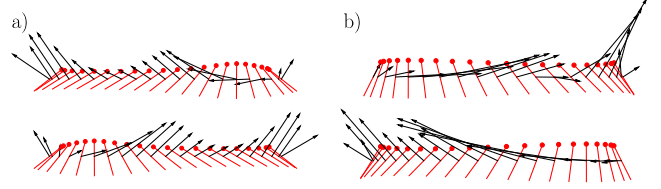

FIG. 2 (color online).   (a) Optimized flapping motion. The optimal flapping motion found here uses 27% less power than the optimal fixed wing kinematics. The aerodynamic power is calculated after steady state is reached by averaging over four periods of motion. (b) Sinusoidal motion [4]. Wing chords [gray (red)] and the aerodynamic force (black) are shown equally spaced in time. The optimized flapping motion in (a) requires only 38% of the aerodynamic power used by the sinusoidal motion in (b) to lift the same weight. We set the amplitude to be the arclength traveled by the wing of a typical fruit fly at $2/3$ of its length, which is about 6 chords, and the profile of the wing velocity to be almost square ($K = 0.9$) as previously found by a quasisteady analysis [5]. A typical fruit fly has a mass $m \approx 1$ mg. Its wing has a radius $r \approx 0.2$ cm, a mean chord $\bar{c} \approx 6.8 \times 10^{-2}$ cm, and a typical flapping frequency of 250 Hz [18,19]. Thus, each wing supports a weight of about 0.5 mg flapping at a Reynolds number of about 100.

Stokes solution with the required accuracy. After the force balance constraint is eliminated by tuning the frequency of motion, the optimization is reduced to an unconstrained problem in the remaining parameters which we solve by using a simple bisection algorithm in each dimension.

First, we determine the optimum among all steady wing motions. A steady wing motion is specified by its velocity U and its angle of attack α [Fig. 1(a)]. Following the procedure described above, for each α, we determine U by satisfying the weight balance constraint. We then determine the minimal power in α. In the range of α between $20°$ and $40°$, containing the optimal angle of attack, the flow around the wing is separated, exhibiting dynamic stall followed by periodic vortex shedding (Fig. 1). The aerodynamic power is calculated by averaging over four periods of motion after steady state is reached. The minimum specific power $P_s = 0.245$ occurs at a velocity of 2.94 m/s and an angle of attack of $27.5°$.

Next, we consider flapping wing motions for the same wing. There are infinite choices of parametrizations for flapping kinematics. It is desirable to describe the flapping motion with a small number of parameters without excluding all of the efficient motions. Following [5], we consider a family of periodic motions based on observed hovering insect wing kinematics [Fig. 2(a)]. The stroke angle $\phi(t)$ is given by a smoothed triangular waveform, parametrized by K, $\phi(t) = \frac{\phi_m}{\sin^{-1} K} \sin^{-1}[K \sin(2\pi f t)]$. The wing pitching angle $\eta(t)$ is given by a periodic hyperbolic function, parametrized by C, $\eta(t) = \frac{\eta_m}{\tanh C_\eta} \tanh[C_\eta \sin(2\pi f t + \Phi_\eta)] + \eta_0$. This parametrization has the advantage of decoupling the relevant aerodynamic features of a flapping motion into separate parameters: the flapping frequency

(f), the amplitude (A), the angle of attack at the midstroke ($\alpha_{\max}$), the speed of turning (K), the speed of rotation of the wing at reversal (C), and the phase between the translation and rotation of the wing (ϕ_0). The wing velocity and angle of attack can smoothly vary between sinusoidal and square profiles with a single parameter.

By optimizing the angle of attack, the speed of turning, and the phase between reversal and pitching while tuning the flapping frequency to satisfy the weigh balance constraint with the procedure described above, we obtain a minimum value of the specific power of $\bar{P}_s = 0.178$ at (f, $\alpha_{\max}$, ϕ) = (218 Hz, 30°, $\pi/4$) (Figs. 2 and 3). This is 27% more efficient than the optimal steady motion, significantly less costly than kinematics previously considered in the literature. For example, sinusoidal kinematics [4] use more than twice the power to lift the same weight, and 70% more compared to the optimal fixed wing motion. To investigate why the optimal flapping motion presented here is more efficient than steady and simple sinusoidal motions, we examine the time dependent aerodynamic force and power shown in Fig. 3. In particular, we focus on two segments: the midstroke and near wing reversal. In contrast with sinusoidal flapping motions where the angle of attack quickly deviates from its optimal value, the midstroke of the optimal flapping motion has an almost constant angle of attack at about 30°, which is near the optimal value for this wing (Fig. 1). This suggests that the main difference between the optimal flapping and the optimal steady motion lies in the unsteady aerodynamics near wing reversal.

Immediately after wing reversal, the vertical force of the optimal flapping motion exhibits a large peak similar to those previously observed in robotic wing experiments [14] (Fig. 4). This large force is produced at a specific power $P_s = 0.1$, much smaller than the specific power during the midstroke. In order to understand how this large force is produced efficiently, we manipulate the flow around the wing in our simulations. In particular, we remove various vortices from the flow after wing reversal to quantify their effects on the fluid force. Specifically, we remove vortices from the wake of the wing by setting the vorticity field to zero in the corresponding regions and connect them to the surrounding vorticity field by a linear interpolation. Since the vortices removed are a few chords away from the wing, the no-slip boundary condition at the wing is unaffected. In addition, because we are working with vorticity field, the incompressibility condition is automatically satisfied. This new vorticity field is then evolved in time. We found that the leading edge vortex generated in the previous stroke has the most significant effect on the subsequent unsteady aerodynamic force. Figure 4 shows the vorticity fields produced under two different conditions: (a) the unperturbed flow after three periods of motion and (b) the flow at the same time as in (a) but with the previous leading edge vortex removed just before the wing reversal, at time $t/T = 2.78$, where T is one period of motion. The main difference in the fluid flow between these two cases is best seen in the velocity field near the wing (Fig. 4). In the unperturbed case (a), after the wing reverses, the flapping wing moves into an effective incoming upward flow of about 2 m/s, resulting in a force of 1.2 mg with an average specific power of 0.1. On the other hand, in (b) the wing moves into a downward flow and the force trace in Fig. 4(c) exhibits no peak following reversal. After about half a period, the force traces in (a) and (b) converge again to the same values. The average forces over a period of motion are 0.5 mg and 0.26 mg for case (a) and (b), respectively, and the corresponding averaged power is 12 μW in both cases. Note that while the unperturbed case is more efficient than the optimal steady motion, this is no longer true in the absence of the leading ledge vortex, which has the specific power of 0.52. Removing other vortices shed during earlier periods of motions had a much smaller effect.

To the best of our knowledge, the optimizations presented here provide the first piece of evidence that, at the
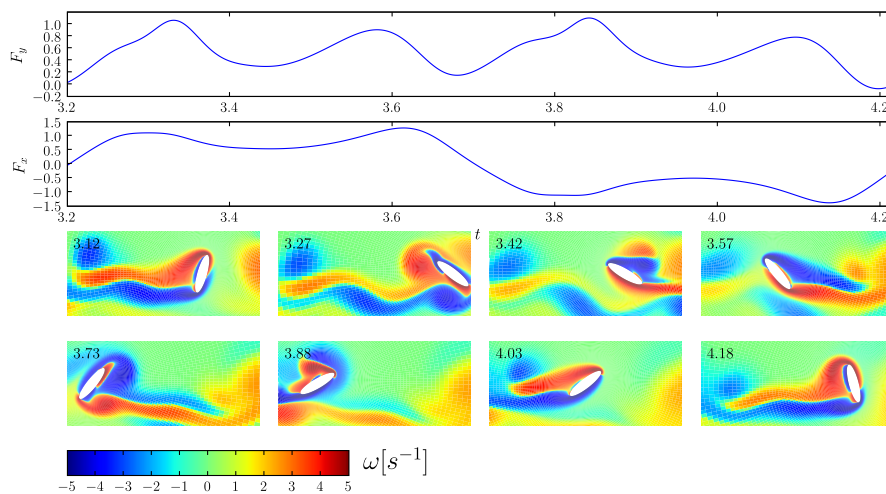

FIG. 3 (color online).   Fluid force (F_x and F_y) and vorticity field (ω) during one period of optimized wing motion.
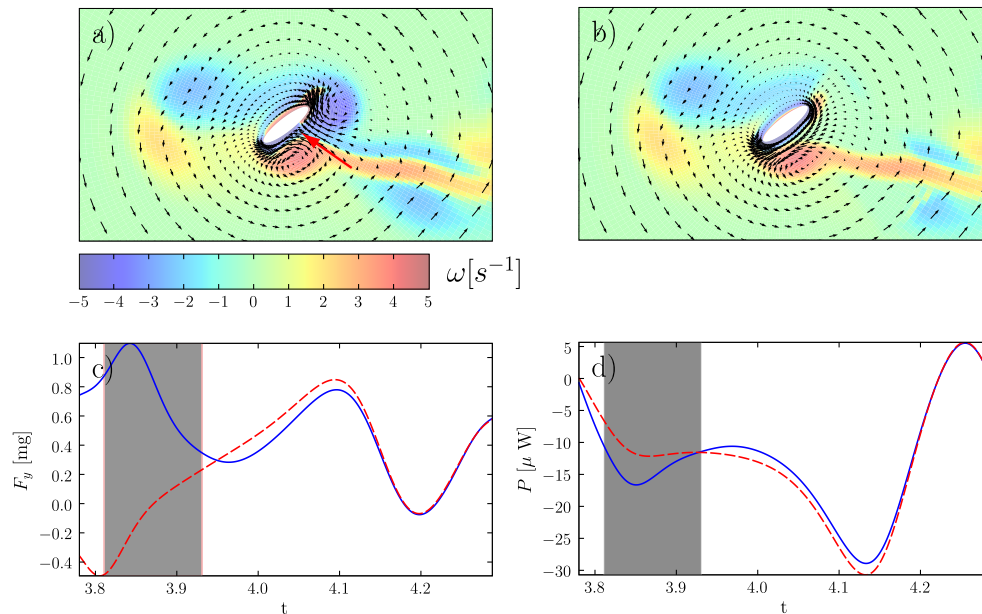
FIG. 4 (color online). Wing-wake interaction near wing reversal. (a) Velocity field immediately after wing reversal in the unperturbed case. (b) Velocity field after the leading edge of the previous stroke has been artificially removed. (c),(d) Vertical force and power for half a period of motion. The traces in solid (blue) lines and dashed (red) lines correspond to the force and power generated by the unperturbed flow in (a) and to the modified flow in (b), respectively. The interaction with the leading edge vortex of the previous stroke increases both the lift and fluid power. However, the net effect is beneficial to the efficiency of lift production, as the lift in the shaded region increases threefold while the required power only increases by 50%.

scale of insects, a two-dimensional flapping flight can be aerodynamically more efficient than the optimal fixed wing flight. This is achieved by taking advantage of the interaction of the wing with its wake near wing reversal. Although the calculation presented here was carried out in 2D, the same methodology can be extended to three dimensions. When future 3D computations are carried out at comparable speed as the current 2D computations, it will be interesting to examine the results from 3D optimization.

Designing small scale flapping devices is an active area of current flapping flight research [15–17]. A notable challenge in designing effective small scale flapping devices is to obtain flight efficiency comparable to fixed wing flight. Current research has focused on improving the efficiency of power source and the design of the wing architecture. Our study suggests that efficiency can be gained significantly by tuning the wing motion.

*Corresponding author.
zw24@cornell.edu

[1] Z. J. Wang, Annu. Rev. Fluid Mech. **37**, 183 (2005).
[2] A. Hedenstrom, V. Griethuijsen, M. Rosen, and G. R. Spedding, Animal biology **56**, 535 (2006).
[3] S. Sane and M. H. Dickinson, J. Exp. Biol. **204**, 2607 (2001).
[4] Z. J. Wang, J. M. Birch, and M. H. Dickinson, J. Exp. Biol. **207**, 449 (2004).
[5] G. Berman and Z. J. Wang, J. Fluid Mech. **582**, 153 (2007).
[6] S. Alben, J. Fluid Mech. **614**, 355 (2008).
[7] S. Kern and P. Koumoutsakos, J. Exp. Biol. **209**, 4841 (2006).
[8] Z. J. Wang, J. Exp. Biol. **211**, 234 (2008).
[9] M. Sun and S. Lan, J. Exp. Biol. **207**, 1887 (2004).
[10] R. Mittal, H. Dong, M. Bozkurttas, G. V. Lauder, and P. Madden, Bioinsp. Biomim. **1**, S35 (2006).
[11] S. Xu and Z. J. Wang, Comput. Methods Appl. Mech. Eng. **197**, 2068 (2008).
[12] Z. J. Wang, Phys. Rev. Lett. **85**, 2216 (2000).
[13] U. Pesavento and Z. J. Wang, Phys. Rev. Lett. **93**, 144501 (2004).
[14] M. H. Dickinson, F. O. Lehmann, and S. P. Sane, Science **284**, 1954 (1999).
[15] R. J. Wood, IEEE Trans. Robot. **24**, 341 (2008)
[16] http://www.delfly.nl; http://www.avinc.com.
[17] W. R. F. van Breugel and H. Lipson, IEEE Robot. Autom. Mag. **15**, 68 (2008).
[18] A. R. Ennos, J. Exp. Biol. **142**, 49 (1989).
[19] S. N. Fry, R. Sayaman, and M. H. Dickinson, J. Exp. Biol. **208**, 2303 (2005).